Expanded View Figures

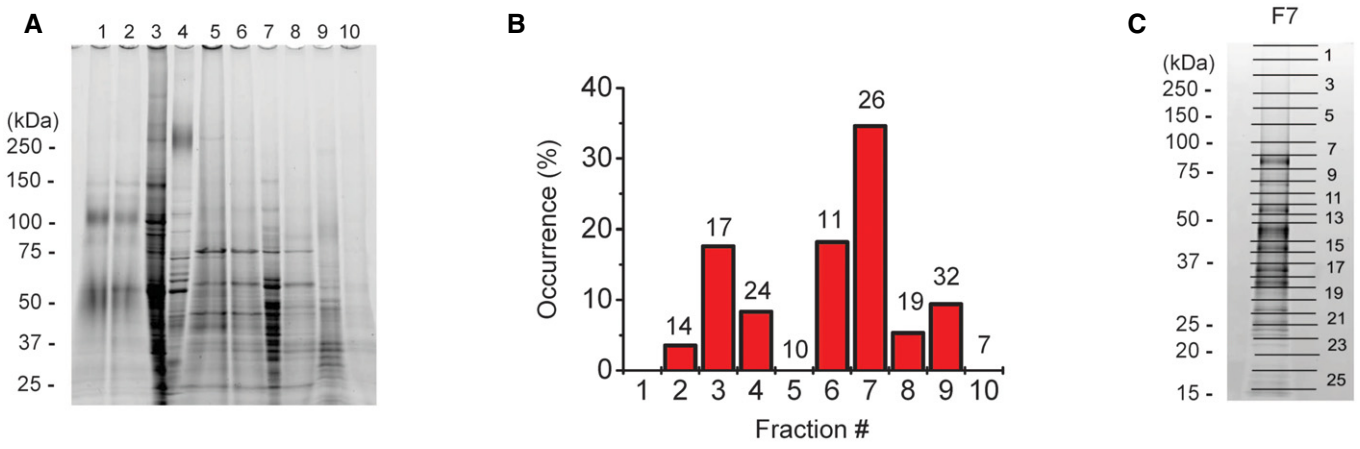

Figure EV1. Fractionation of the bleb-membrane proteins.

A SDS–PAGE electrophoresis of the protein fractions obtained after preparative liquid-phase isoelectric focusing.

B Maxi-Cl activity in each fraction after reconstitution into the giant liposomes. Number of patches tested is shown at the top of each column. No proteoliposomes could be formed using fraction-1.

C The gel for F7 was divided into 26 pieces for the LC-MS/MS analysis.

Source data are available online for this figure.

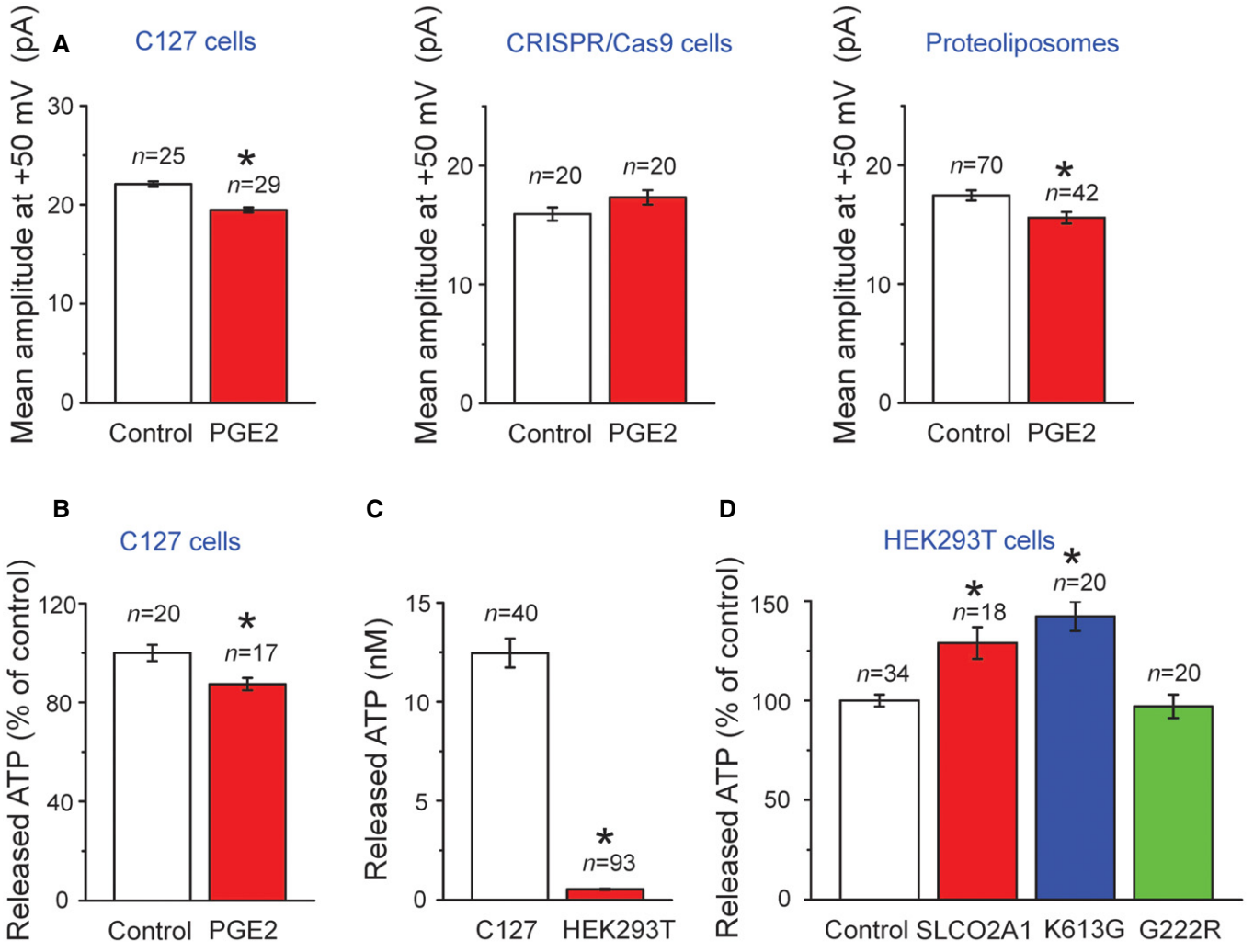

Figure EV2. Effects of PGE2 on single maxi-anion currents and on swelling-induced ATP release from C127 cells as well as effects of overexpression with SLCO2A1 and its mutants on swelling-induced ATP release from HEK293T cells.

A Averaged single-channel amplitudes recorded at +50 mV in patches excised from C127 cells (left graph, n = 25 for Control and 29 for PGE2), from CRISPR/Cas9 KO C127 cells (center graph, n = 20 for Control and 20 for PGE2), and from giant proteoliposomes with reconstituted recombinant SLCO2A1 protein (right graph, n = 70 for Control and 42 for PGE2) in the absence (Control) and presence of 20 μM PGE2 added to bath and pipette solutions. The data from 4 to 9 cells and 4 proteoliposomes for each value are pooled.

B Swelling-induced ATP release from C127 cells in the absence (Control, n = 20) and presence of 20 μM PGE2 (n = 17). To test PGE2 effects, the cells were pre-incubated with Ringer solution containing PGE2 and challenged with hypotonic medium containing PGE2.

C Comparison between the absolute level of the swelling-induced ATP release from (n = 40) and that from HEK293T cells (n = 93).

D Swelling-induced release of ATP from HEK293T cells transfected with mock (Control, n = 34)), WT SLCO2A1(n = 18) or with the mutants K613G (n = 20) and G222R (n = 20; see Appendix Table S2 for the expression vectors used here).

Data information: Error bars, SEM. * indicates significantly different from Control C127 cells (A–C, by Student's t-test) or mock-transfected Control HEK293T cells (D, by ANOVA) at $P < 0.05$.

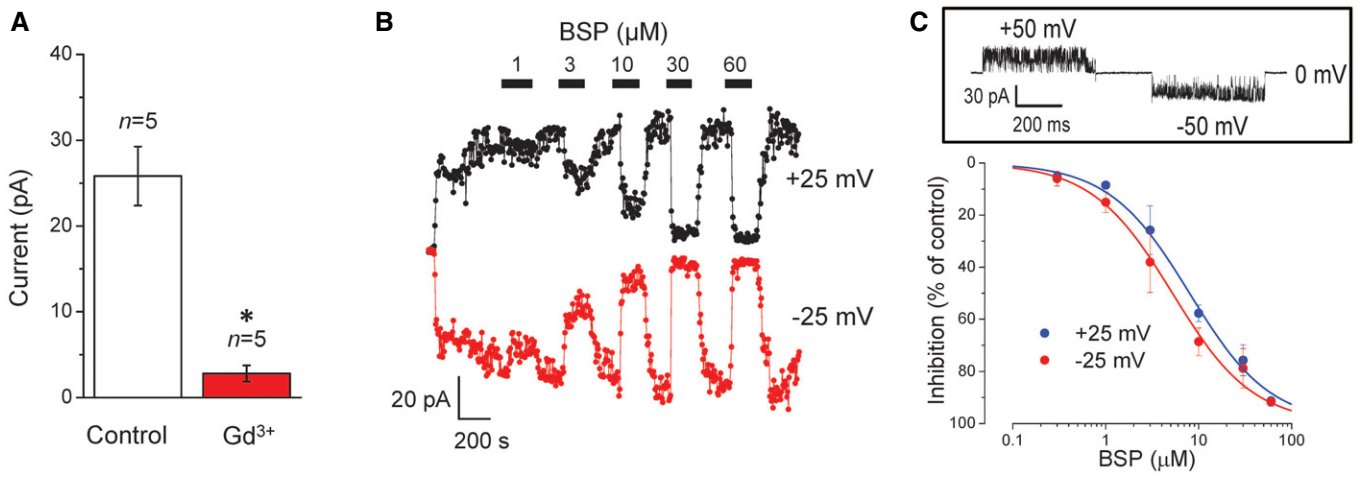

Figure EV3. Gd^{3+} and BSP sensitivity of non-Maxi-Cl channels in SLCO2A1-deficient cells.

A Mean patch currents recorded at +25 mV in the outside-out mode in the absence (Control: white column) and presence of Gd^{3+} (50 μM: red column) in the bath solution. Error bars, SEM, *$P < 0.05$ (Student's *t*-test). $n = 5$ (from different cells) for Control and Gd^{3+}.

B Dose-dependent inhibitory effects of BSP (added at bars) on currents recorded from an inside-out patch in response to a step-pulse of ±25 mV applied every 5 s. Result of the representative experiment is shown.

C Concentration–response curves of BSP effects with IC_{50} = 8.3 ± 1.7 μM at +25 mV and 5.2 ± 0.4 μM at −25 mV. The inset on top shows flickery currents observed in the presence of 3 μM BSP. $n = 5$ for each data point (from five different experiments as shown on panel B). Error bars, SEM.

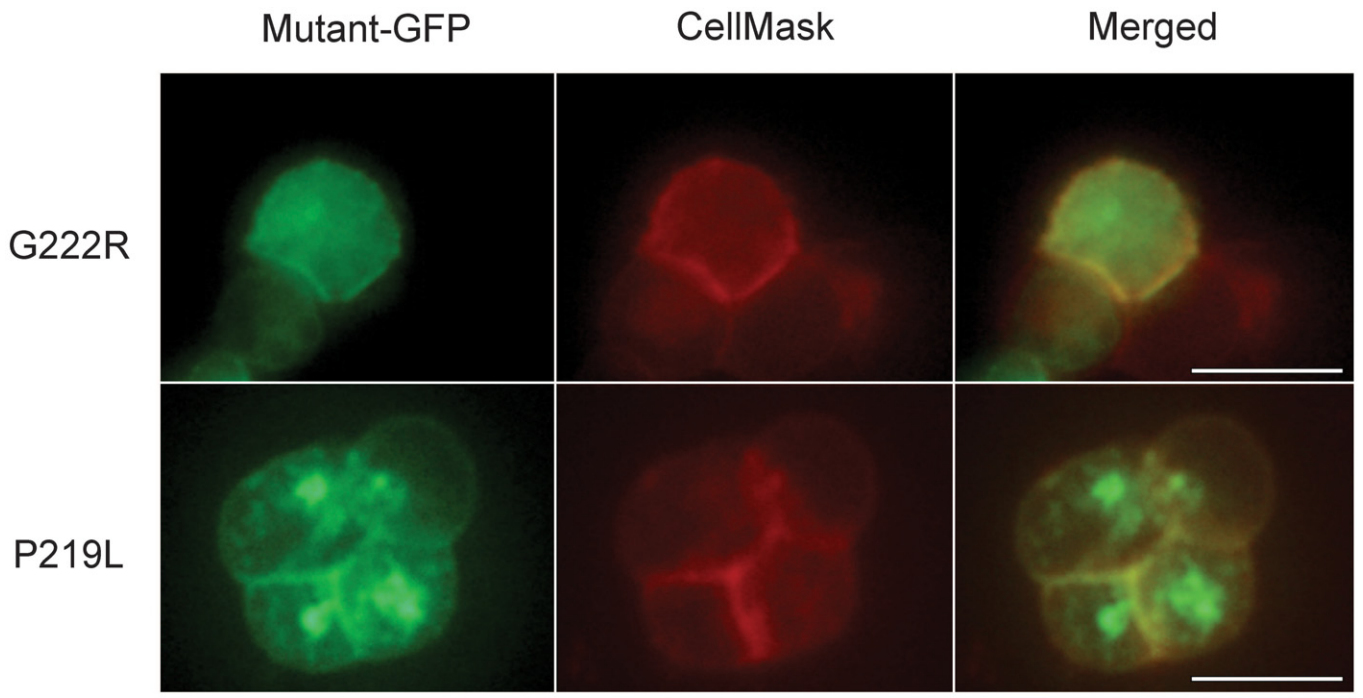

Figure EV4. Localization of GFP-tagged G222R mutant (upper row) and P219L mutant (lower row) proteins.

Mutant-transfected HEK293T cells were stained with CellMask™ Orange Plasma Membrane Stain (CellMask) and observed under a fluorescence microscope; scale bars, 10 μm.

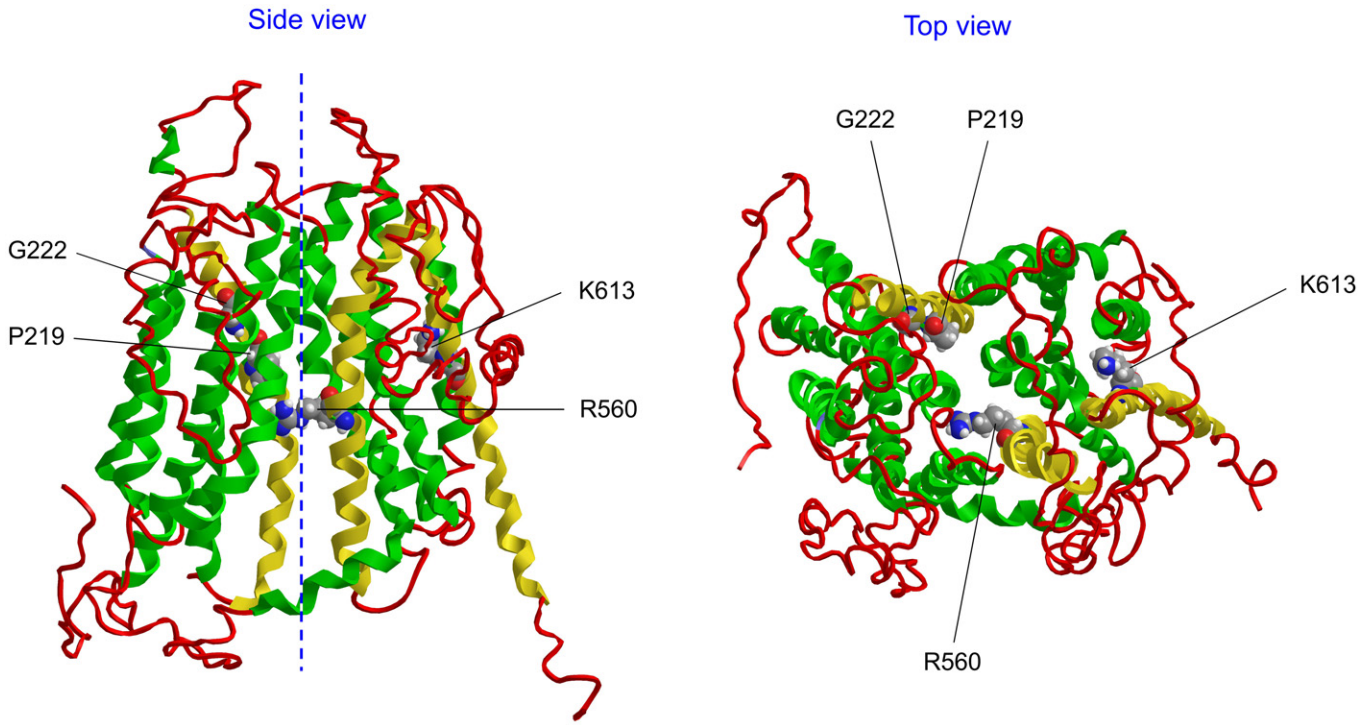

Figure EV5. Homology model of the wild-type SLCO2A1 protein.

The model was built using I-TASSER (Iterative Threading ASSEmbly Refinement) server (http://zhanglab.ccmb.med.umich.edu/I-TASSER/). The server selected the crystal structure of the glycerol-3-phosphate transporter from *Escherichia coli* (PDB ID: 1PW4A) as the best template.

A A Side view. The dashed line marks the central axis of the molecule. Amino acids for the mutations which are discussed in the text are highlighted and indicated. The transmembrane helixes bearing these amino acids are colored in yellow. Other helixes are shown in green.

B Top view.